


# Accurate determination of energy levels, hyperfine structure constants, lifetimes and dipole polarizabilities of triply ionized tin isotopes

Mandeep Kaur<sup>1</sup>, Rishabh Nakra<sup>1</sup>, Bindiya Arora<sup>1</sup>, Cheng-Bin Li<sup>2</sup> and B K Sahoo<sup>3,4</sup> 

<sup>1</sup> Department of Physics, Guru Nanak Dev University, Amritsar, Punjab-143005, India

<sup>2</sup> State Key Laboratory of Magnetic Resonance and Atomic and Molecular Physics, Wuhan Institute of Physics and Mathematics, Chinese Academy of Sciences, Wuhan 430071, People's Republic of China

<sup>3</sup> Atomic, Molecular and Optical Physics Division, Physical Research Laboratory, Navrangpura, Ahmedabad-380009, India

E-mail: [bindiya.phy@gndu.ac.in](mailto:bindiya.phy@gndu.ac.in), [cbli@wipm.ac.cn](mailto:cbli@wipm.ac.cn) and [bijaya@prl.res.in](mailto:bijaya@prl.res.in)

Received 30 June 2019, revised 3 December 2019

Accepted for publication 7 January 2020

Published 24 February 2020



CrossMark

## Abstract

We have investigated the energies, magnetic dipole hyperfine structure constants ( $A_{hyf}$ ) and electric dipole (E1) matrix elements of a number of low-lying states of triply ionized tin ( $\text{Sn}^{3+}$ ) by employing relativistic coupled-cluster theory. Contributions from the Breit interaction and lower-order quantum electrodynamic (QED) effects in the determination of the above quantities are also given explicitly. These higher-order relativistic effects are found to be important for the accurate evaluation of energies, while only QED contributions are seen to contribute significantly to the determination of  $A_{hyf}$  values. Our theoretical results for the energies are in agreement with one of the measurements but show significant differences for some states with another measurement. Reported  $A_{hyf}$  will be useful in guiding the measurements of hyperfine levels in the stable isotopes of  $\text{Sn}^{3+}$ . The calculated E1 matrix elements are further used to estimate the oscillator strengths, transition probabilities and dipole polarizabilities ( $\alpha$ ) of many states. Large discrepancies between the present results and previous calculations of oscillator strengths and transition probabilities are observed among a number of states. The estimated  $\alpha$  values will be useful for carrying out high precision measurements using the  $\text{Sn}^{3+}$  ion in future experiments.

Supplementary material for this article is available [online](#)

Keywords: atomic structure, fine and hyperfine splitting, polarizability, QED correction, coupled-cluster

## 1. Introduction

The spectra of medium to highly charged ions have aroused considerable interest in recent years for their applications in fundamental physics, such as in the search for the variation of fundamental constants [1], the development of high precision

optical frequency standards [2–4], establishing a very long-baseline interferometer for telescope array synchronization, the development of extremely sensitive quantum tools for geodesy [5, 6] and astronomy [7, 8]. Spectroscopic investigations of  $\text{Sn}^{3+}$  ions have been an attractive research topic in plasma physics because of their potential use in laser-produced plasmas (LPPs) to generate standard laboratory ion sources [9–11] and pulsed short wavelength light sources

<sup>4</sup> Author to whom any correspondence should be addressed.

[12]. LPPs have abundant applications in extreme-ultraviolet (EUV) lithography [13, 14], EUV metrology [15] and surface treatment and modification [16]. Spectroscopic information, such as the study of line strengths for  $\text{Sn}^{3+}$ , can help in predicting the optimum plasma parameters and experimental conditions for the production of laser-produced Sn plasma sources [17, 18]. Despite the well-understood nature of the force that binds these charged ions, highly accurate calculations of their properties are difficult and relatively sparse. In the present work, we have considered medium charged  $\text{Sn}^{3+}$  ions from a Ag-like isoelectronic sequence for the theoretical investigation of various spectroscopic properties. For this ion, both Coulomb interactions and relativistic effects will be equally important in accurately obtaining its properties. We have carried out calculations by including these interactions with relativistic coupled-cluster (RCC) theory.

The theoretical calculations and measurements of the energies of the ground and some low-lying states of  $\text{Sn}^{3+}$  are available in the literature [19–24]. Scheers *et al* [19] obtained the optical spectra of  $\text{Sn}^{3+}$  from a laser-produced plasma. In the same work, they also made relativistic Fock-space coupled-cluster (FSCC) calculations of the measured energy levels. Su *et al* [25] has performed the evolutionary analysis of EUV radiation from laser-produced Sn plasmas. They had applied the configuration interaction (CI) method using the Cowan code to generate the required atomic data for the spectral analysis and simulation. Safronova *et al* [26] has presented Ag-like isoelectronic sequences and showed that they satisfy the criteria for experimental exploration in many fields of physics. Safronova *et al* [24] used relativistic many-body perturbation theory (RMBPT method) to determine the energies and lifetimes of the  $4F_j$ ,  $5P_j$  and  $5D_j$  states in  $\text{Sn}^{3+}$ . Only a few spectroscopic studies of some of the low lying states of  $\text{Sn}^{3+}$  have been carried out [24, 27, 28]. Safronova *et al* [24] has determined the oscillator strengths for the  $5S_j - 5P_j$ ,  $5P_j - 5D_j$ ,  $4F_j - 5D_j$  and  $4F_j - 5G_j$  transitions using the RMBPT method. Biswas *et al* [27] has estimated the transition properties for 33 lines of  $\text{Sn}^{3+}$  using RCC theory. In their analysis, corrections due to Briet and quantum electrodynamic (QED) effects, such as the electron self-energy and vacuum polarization interactions, were omitted. The oscillator strengths of a few transitions are given by Cheng and Kim [28] using the multi-configuration Dirac–Fock method. There have been a few measurements of the lifetimes of some of the states of  $\text{Sn}^{3+}$  [29–31] using the beam foil technique. Lifetime calculations of a few excited states of  $\text{Sn}^{3+}$  have been made by Cheng *et al* [28] using the relativistic Hartree–Fock method and by Pinnington *et al* [31] using Coulomb approximation.

The study of hyperfine structure constants is of immense interest for several applications. The accurate determination of these quantities provides a stringent test of the correct behavior of calculated atomic wave functions in the nuclear region [32–35]. They are also employed to test the potential of many-body methods by reproducing the measured values at different levels of approximations in the employed methods [34–36]. One can infer nuclear moments by combining measured hyperfine

structure constants with the corresponding calculations [35, 36]. Accurate investigation of these quantities is essential to estimate the Zeeman shifts of the atomic energy levels in high-precision experiments [3, 4, 37–39]. Tolansky and Forester [40] have studied hyperfine structure splittings in the arc spectra of tin and confirmed that the two odd isotopes of tin, Sn (117) and Sn (119), have nuclear spin 1/2 and an identical magnetic moment. However, measurements of the hyperfine structure constants of the Sn IV ion for any isotope are not available so far.

In this work, we intend to investigate the roles of the electron correlation effects and higher-order relativistic corrections using RCC theory for the accurate calculation of various properties in  $\text{Sn}^{3+}$ . For this purpose, we present the energies and magnetic dipole hyperfine structure constants ( $A_{hyf}$ ) of the  $nS_{1/2}$  ( $n = 5 - 9$ ),  $nP_{1/2,3/2}$  ( $n = 5 - 9$ ),  $nD_{3/2,5/2}$  ( $n = 5 - 9$ ) and  $nF_{5/2,7/2}$  ( $n=4,5$ ) states of  $\text{Sn}^{3+}$ . The accurate determination of  $A_{hyf}$  values is very sensitive to relativistic effects owing to its origin from the atomic nucleus [41]. We have also determined the electric dipole (E1) matrix elements among the above states. Using these elements, we further determine the transition probabilities and oscillator strengths for many transitions. Additionally, we estimate the lifetimes and static dipole polarizabilities of many states. A comparison between some of our calculations and other experimental and theoretical values available in the literature is also presented. The spectroscopic investigations of the Sn ion carried out in this work have potential applications in future thermonuclear fusion reactors [42–44] and their discovery in various stellar and interstellar atmospheres [45–51]. Our results on  $A_{hyf}$  values and dipole polarizabilities will be useful for the comprehensive understanding of the roles of electron correlation effects and higher-order relativistic effects in their determination by comparing them with the experimental values when available in the future. In sections 2, 3 and 4, we present the theory and method of the calculations, the results and discussion, and the conclusions, respectively.

## 2. Theory and method of calculations

### 2.1. RCC theory

We use RCC theory with the single and double excitations approximation (RCCSD method) (for example, see [52–54]) to determine the wave functions of the ground and excited states of the  $\text{Sn}^{3+}$  ion. In this approach, we first obtain the Dirac–Hartree–Fock (DHF) wave function ( $|\Phi_0\rangle$ ) for the closed core of  $\text{Sn}^{4+}$ , then append the respective valence orbital ( $v$ ) of the ground or excited state as  $|\Phi_v\rangle = a_v^\dagger |\Phi_0\rangle$  to define the DHF wave function of  $\text{Sn}^{3+}$  (also known as the  $V^{N-1}$  potential). Considering this DHF wave function as the starting point, the exact atomic wave function ( $|\Psi_v\rangle$ ) is determined by expressing it in RCC theory as

$$|\Psi_v\rangle = e^T \{1 + S_v\} |\Phi_v\rangle, \quad (1)$$

where the RCC operators  $T$  and  $S_v$  are responsible for carrying out excitations of the core, and core and valence electrons

**Table 1.** The calculated excitation energy values using the DHF and RCCSD methods for the valence orbitals of  $\text{Sn}^{3+}$  (in  $\text{cm}^{-1}$ ) are presented. The ‘total’ column lists the sum of the RCCSD calculations including Breit interaction ( $\delta_{\text{Breit}}$ ) and QED effects ( $\delta_{\text{QED}}$ ). A comparison with the theoretical values using relativistic many-body perturbation theory (RMBPT) calculations [24] and Fock space coupled-cluster (FSCC) calculations [19] is given. The experimental values obtained in [19, 22] and [23] are compared. Uncertainties are presented in parentheses whereas only statistical uncertainty is presented in parentheses for the experimental results from [19]. The BE values from the RCCSD method are also given at the bottom.

State	This work					Others		Experiment	
	DHF	RCCSD	$\delta_{\text{Breit}}$	$\delta_{\text{QED}}$	Total	RMBPT [24]	FSCC [19]	[19]	[22, 23]
$5S_{1/2}$	0	0	0	0	0	0	0	0	0 [23]
$5P_{1/2}$	66 323.692	69 681.368	49.589	−90.275	69641(1185)	69265	69741		69 563.9 [23]
$5P_{3/2}$	72 291.712	76 261.815	−34.819	−111.78	76115(1166)	75736	76256		76 072.3 [23]
$5D_{3/2}$	156 482.544	165 698.24	−132.933	−104.872	165460(1011)	164538	165646	165304(1)	165 304.7 [23]
$5D_{5/2}$	157 181.818	166 453.354	−153.345	−107.002	166193(1005)	165283	166382	165409(1)	165 410.8 [23]
$6S_{1/2}$	164 598.765	174 156.834	−104.916	−74.952	173977(1012)		174236	174 138.8(4)	174 138.8 [23]
$6P_{1/2}$	187 743.537	197 934.886	−83.068	−100.339	197751(992)		198025	197 850.6(6)	197 850.9 [23]
$6P_{3/2}$	189 845.187	200 151.587	−110.882	−107.274	199933(990)		200216	200 030.1(4)	200 030.8 [23]
$4F_{7/2}$	200 700.345	210 868.219	−164.418	−104.108	210599(993)	209418	210554	210 258.2(6)	210 257.7 [23]
$4F_{5/2}$	200 786.473	210 938.307	−163.149	−104.165	210671(993)	209494	210627	210 317.9(7)	210 318.2 [23]
$6D_{3/2}$	223 348.684	236 059.541	−140.896	−102.866	235816(1382)		235171	234 797.0(1)	234 795.7 [23]
$6D_{5/2}$	223 665.869	236 367.216	−149.822	−106.37	236111(1364)		235497	235 128.7(2)	235 127.7 [23]
$7S_{1/2}$	226 054.02	237 657.685	−130.047	−91.767	237436(975)		237920	237617(1)	237 615.7 [23]
$7P_{1/2}$	237 033.876	248 820.864	−118.438	−102.859	248599(973)		249094	248 735.4(2)	
$7P_{3/2}$	238 045.388	249 868.557	−131.362	−106.214	249631(972)		250233	249 644.8(1)	
$5F_{7/2}$	241 131.954	252 545.707	−164.005	−134.164	252247(984)	250981	252626	251 853.0(2)	
$5F_{5/2}$	241 187.899	252 527.244	−160.734	−86.885	252279(977)	251025	252666	252 162.6(2)	
$7D_{3/2}$	255 004.484	267 331.238	−146.097	−105.2	267080(969)		267475	267 215.5(2)	267 247.6 [22]
$7D_{5/2}$	255 175.107	267 511.929	−151.017	−105.746	267255(969)		267647	267 394.7(2)	267 395.7 [22]
$8S_{1/2}$	256 302.957	268 626.54	−139.473	−97.969	268389(970)		268895	268 544.3(3)	268544 [22]
$8P_{1/2}$	262 466.314	275 420.271	−133.151	−104.215	275183(967)				
$8P_{3/2}$	263 042.548	276 008.39	−140.286	−105.939	275762(967)				
$8D_{3/2}$	272 725.583	285 391.723	−147.942	−105.057	285139(968)		285497	285865(1)	
$8D_{5/2}$	272 826.052	285 497.679	−150.815	−105.529	285241(968)		285597	285370(1)	
$9S_{1/2}$	273 685.822	286 303.296	−143.41	−100.542	286059(968)				286013 [22]
$9P_{1/2}$	277 722.569	290 763.335	−138.309	−104.466	290520(967)				
$9P_{3/2}$	278 133.263	291 184.229	−143.06	−105.699	290935(967)				
$9D_{3/2}$	283 870.151	296 762.238	−149.197	−105.215	296508(967)				
$9D_{5/2}$	283 923.004	296 817.943	−150.71	−105.383	296562(967)				
BE	315 810.897	328 953.136	−150.639	−105.221	328697(967)	327453	328999	328 908.4(3)	328550(300) [23] 328910 [22]

respectively from the DHF wave functions due to the correlation effects. In the RCCSD method, these RCC operators can be given in the second quantization notation as

$$T = \sum_{a,p} \eta_a^p a_p^\dagger a_a + \frac{1}{4} \sum_{a,b,p,q} \eta_{ab}^{pq} a_p^\dagger a_q^\dagger a_b a_a \quad (2)$$

and

$$S_v = \sum_{p \neq v} \eta_v^p a_p^\dagger a_v + \frac{1}{2} \sum_{p,q,a} \eta_{va}^{pq} a_p^\dagger a_q^\dagger a_a a_v, \quad (3)$$

where  $a$ ,  $b$  and  $p$ ,  $q$  indices represent the occupied and unoccupied orbitals, respectively, and  $\eta$  represents the corresponding excitation amplitudes. These amplitudes are solved by using the following equations

$$\langle \Phi_0^K | \bar{H}_N | \Phi_0 \rangle = \delta_{K,0} (E_0 - E_{DHF}), \quad (4)$$

and

$$\langle \Phi_v^L | \bar{H}_N \{1 + S_v\} | \Phi_v \rangle = (E_v - E_0) \langle \Phi_v^L | \{\delta_{L,0} + S_v\} | \Phi_v \rangle, \quad (5)$$

where  $\bar{H}_N \equiv e^{-T} H e^T$  with the atomic Hamiltonian  $H$  and subscript  $N$  means normal order form with respect to the reference state  $|\Phi_0\rangle$ . The superscripts  $K$  and  $L$  indicate  $K$ th and  $L$ th excited determinants with respect to  $|\Phi_0\rangle$  and  $|\Phi_v\rangle$ , respectively. Here,  $E_{DHF}$  and  $E_0$  are the DHF and total energies of the closed core, and  $E_v$  is the total energy of the considered state of  $\text{Sn}^{3+}$  containing the valence orbital  $v$ . Therefore, the evaluation of  $E_v - E_0$  will give the binding energies (BE) to  $\text{Sn}^{4+}$  for the corresponding valence orbital  $v$ . The excitation energies (EEs) between different states are estimated by taking the differences of the BE values of the associated states.

## 2.2. Construction of the Hamiltonian

For the calculations, we consider first the Dirac–Coulomb (DC) Hamiltonian given by

$$H^{DC} = \sum_i [c \boldsymbol{\alpha}_i \cdot \mathbf{p}_i + (\beta_i - 1)c^2 + V_n(r_i)] + \sum_{i,j>i} \frac{1}{r_{ij}}, \quad (6)$$

where  $c$  is the speed of light,  $\boldsymbol{\alpha}$  and  $\beta$  are the usual Dirac matrices,  $\mathbf{p}_i$  is the single particle momentum operator,  $V_n(r_i)$  denotes the nuclear potential, and  $\frac{1}{r_{ij}}$  represents the Coulomb potential between the electrons located at the  $i$ th and  $j$ th positions.

We investigate the Breit interaction contribution by including the following potential in the DC Hamiltonian (defined as the DCB Hamiltonian)

$$V^B = - \sum_{j>i} \frac{[\boldsymbol{\alpha}_i \cdot \boldsymbol{\alpha}_j + (\boldsymbol{\alpha}_i \cdot \mathbf{r}_{ij})(\boldsymbol{\alpha}_j \cdot \mathbf{r}_{ij})]}{2r_{ij}}, \quad (7)$$

where  $\mathbf{r}_{ij}$  is the unit vector along  $\mathbf{r}_{ij}$ .

Contributions from the QED effects are estimated by considering the lower-order vacuum polarization (VP) interaction ( $V_{VP}$ ) and the self-energy (SE) interactions ( $V_{SE}$ ). We

account for  $V_{VP}$  through the Uehling [55] and Wichmann–Kroll potentials ( $V_{VP} = V^{Ueh} + V^{WK}$ ) given by

$$V^{Ueh} = -\frac{2}{3} \sum_i \frac{\alpha_e^2}{r_i} \int_0^\infty dx x \rho_n(x) \int_1^\infty dt \sqrt{t^2 - 1} \times \left( \frac{1}{t^3} + \frac{1}{2t^5} \right) [e^{-2ct|r_i-x|} - e^{-2ct(r_i+x)}] \quad (8)$$

and

$$V^{WK} = \sum_i \frac{0.368Z^2}{9\pi c^3(1 + (1.62cr_i)^4)} \rho_n(r_i), \quad (9)$$

respectively, with the electron density over the nucleus as  $\rho_n(r)$  and the atomic number of the system as  $Z$ .

The SE contribution  $V_{SE}$  is estimated by including two parts as

$$V_{SE}^{ef} = -A_l \sum_i \frac{2\pi Z \alpha_e^3}{r_i} I_1^{ef}(r_i) + B_l \sum_i \frac{\alpha_e}{r_i} I_2^{ef}(r_i) \quad (10)$$

known as the effective electric form factor part and

$$V_{SE}^{mg} = \sum_k \frac{i\alpha_e^3}{4} \boldsymbol{\gamma} \cdot \nabla_k \frac{1}{r_k} \int_0^\infty dx x \rho_n(x) \int_1^\infty dt \frac{1}{t^3 \sqrt{t^2 - 1}} \times [e^{-2ct|r_k-x|} - e^{-2ct(r_k+x)} - 2ct(r_k + x - |r_k - x|)], \quad (11)$$

known as the effective magnetic form factor part. In the above expressions, we use [56]

$$A_l = \begin{cases} 0.074 + 0.35Z\alpha_e & \text{for } l = 0, 1 \\ 0.056 + 0.05Z\alpha_e + 0.195Z^2\alpha_e^2 & \text{for } l = 2, \end{cases} \quad (12)$$

and

$$B_l = \begin{cases} 1.071 - 1.97x^2 - 2.128x^3 + 0.169x^4 & \text{for } l = 0, 1 \\ 0 & \text{for } l \geq 2. \end{cases} \quad (13)$$

The integrals are given by

$$I_1^{ef}(r) = \int_0^\infty dx x \rho_n(x) [(Z|r - x + 1|)e^{-Z|r-x|} - (Z(r+x) + 1)e^{-2ct(r+x)}] \quad (14)$$

and

$$I_2^{ef}(r) = \int_0^\infty dx x \rho_n(x) \int_1^\infty dt \frac{1}{\sqrt{t^2 - 1}} \left\{ \left( 1 - \frac{1}{2t^2} \right) \times \left[ \ln(t^2 - 1) + 4 \ln \left( \frac{1}{Z\alpha_e} + \frac{1}{2} \right) \right] - \frac{3}{2} + \frac{1}{t^2} \right\} \times \left\{ \frac{\alpha_e}{t} [e^{-2ct|r-x|} - e^{-2ct(r+x)}] + 2r_A e^{2r_A ct} \times [E_1(2ct(|r-x| + r_A)) - E_1(2ct(r+x + r_A))] \right\} \quad (15)$$

with the orbital quantum number  $l$  of the system,  $x = (Z - 80)\alpha_e$ ,  $r_A = 0.07Z^2\alpha_e^3$ , and the exponential integral  $E_1(r) = \int_r^\infty ds e^{-s}/s$ . We have used the Fermi nuclear charge

**Table 2.** The calculated  $A_{hyf}$  values of many low-lying states of  $^{115}\text{Sn}^{3+}$  (in MHz) from the DHF and RCCSD methods are presented using the DC Hamiltonian. Corrections from the Breit interaction ( $\delta_{Breit}$ ) and QED effects ( $\delta_{QED}$ ) from the RCCSD method are also quoted. Rough estimations of the uncertainties from partial excitations to some of the final results are given in parentheses. We have used  $g_I = -1.837\ 66$  here.

State	DHF	RCCSD	$\delta_{Breit}$	$\delta_{QED}$	Final
$5S_{1/2}$	-35 859.61	-42 415.600	-18.707	357.388	-42077(165)
$5P_{1/2}$	-7 573.95	-9 129.899	11.595	13.267	9105(28)
$5P_{3/2}$	-1 169.13	-1 515.021	-2.444	0.808	-1516(7)
$5D_{3/2}$	-275.15	-395.170	-1.525	0.110	-397.0
$5D_{5/2}$	-115.07	-164.838	-0.772	-0.018	-165.0
$6S_{1/2}$	-10 843.09	-12 324.836	-9.298	100.152	-12233(37)
$6P_{1/2}$	-2 626.56	-3 025.854	1.893	4.135	-3019(9)
$6P_{3/2}$	-414.11	-522.005	-0.992	0.331	-522(6)
$4F_{7/2}$	-9.77	15.730	0.074	0.147	16.0
$4F_{5/2}$	-17.51	-20.269	-0.037	0.165	-20.0
$6D_{3/2}$	-125.65	-139.974	-0.643	0.183	-140.0
$6D_{5/2}$	-52.57	-59.209	-0.147	0.036	-59.0
$7S_{1/2}$	-4 895.78	-5 489.274	-4.722	44.159	-5450(15)
$7P_{1/2}$	-1 259.14	-1 421.503	0.459	1.801	-1419(6)
$7P_{3/2}$	-199.97	-251.208	-0.533	1.065	-250(4)
$5F_{7/2}$	-7.69	10.878	$\sim 0$	$\sim 0$	11.0
$5F_{5/2}$	-13.85	-27.123	-0.111	$\sim 0$	-27.0
$7D_{3/2}$	-67.80	-88.869	-0.349	-0.018	-89.0
$7D_{5/2}$	-28.39	-40.469	-0.165	0.018	-40.0
$8S_{1/2}$	-2 656.68	-2 960.047	-2.738	23.669	-2939(8)
$8P_{1/2}$	-716.76	-762.923	0.551	1.084	-761.0
$8P_{3/2}$	-113.97	-130.363	-0.221	0.055	-131.0
$8D_{3/2}$	-39.98	-52.097	-0.202	$\sim 0$	-52.0
$8D_{5/2}$	-16.77	-23.577	-0.092	$\sim 0$	-24.0
$9S_{1/2}$	-1 717.03	-1 909.328	-1.819	15.234	-1896(4)
$9P_{1/2}$	-513.05	-544.645	4.153	0.772	-540.0
$9P_{3/2}$	-80.80	-90.651	-0.624	0.368	-91.0
$9D_{3/2}$	-21.05	-27.509	-0.110	$\sim 0$	-28.0
$9D_{5/2}$	-8.83	-12.367	-0.055	$\sim 0$	-12.0

distribution in our calculations by defining

$$\rho_n(r) = \frac{\rho_0}{1 + e^{\frac{r-b}{a}}}, \quad (16)$$

for the normalization factor  $\rho_0$ , the half-charge radius  $b$ , and  $a = 2.3/4(\ln 3)$  is related to the skin thickness. We have determined  $b$  using the relation

$$b = \sqrt{\frac{5}{3}r_{rms}^2 - \frac{7}{3}a^2\pi^2}, \quad (17)$$

with the root mean square (rms) charge radius of the nucleus evaluated by using the formula

$$r_{rms} = 0.836A^{1/3} + 0.570, \quad (18)$$

in fm for the atomic mass  $A$ . Our calculations are carried out after including the above QED effects with the DC Hamiltonian (referred to as the DCQ Hamiltonian).

### 2.3. Property evaluation

After obtaining the amplitudes of the RCC operators using equations (4) and (5), we evaluate the reduced matrix elements of an operator between states  $|\Psi_k\rangle$  and  $|\Psi_i\rangle$  from the

following RCC expression

$$\begin{aligned} \langle O \rangle_{ki} &= \frac{\langle \Psi_k | \mathbf{O} | \Psi_i \rangle}{\sqrt{\langle \Psi_k | \Psi_k \rangle \langle \Psi_i | \Psi_i \rangle}} \\ &= \frac{\langle \Phi_k | \{1 + S_k^\dagger\} \bar{\mathbf{O}} \{1 + S_i\} | \Phi_i \rangle}{\sqrt{N_k N_i}}, \end{aligned} \quad (19)$$

where  $\bar{\mathbf{O}} = e^{T^\dagger} \mathbf{O} e^T$  and  $N_v = \langle \Phi_v | e^{T^\dagger} e^T + S_v^\dagger e^{T^\dagger} e^T S_v | \Phi_v \rangle$ . For the evaluation of the expectation value, both the states are taken to be the same. The calculation procedures of these expressions are discussed in detail elsewhere [53, 54]. Next, we discuss the calculations of the hyperfine structure constants, transition probabilities, lifetimes and dipole polarizabilities of the low-lying states of the  $\text{Sn}^{3+}$  ion using the above expression.

**2.3.1. Hyperfine structure constant.** For isotopes with nuclear spin  $I = 1/2$ , the hyperfine levels of an atomic state  $|\Psi_v\rangle$  can be expressed as

$$W_{F,J} = \frac{1}{2} A_{hyf} [F(F+1) - I(I+1) - J(J+1)]. \quad (20)$$

**Table 3.** The calculated  $A_{hyf}$  values of many low-lying states of  $^{117}\text{Sn}^{3+}$  (in MHz) from the DHF and RCCSD methods are presented using the DC Hamiltonian. Corrections from the Breit interaction ( $\delta_{Breit}$ ) and QED effects ( $\delta_{QED}$ ) from the RCCSD method are also quoted. Rough estimations of the uncertainties from partial excitations to some of the final results are given in parentheses. We have used  $g_I = -2.002\ 14$  here.

State	DHF	RCCSD	$\delta_{Breit}$	$\delta_{QED}$	Final
$5S_{1/2}$	-39 069.23	-46 212.014	-20.382	389.376	-45843(180)
$5P_{1/2}$	-8 251.86	-9 947.072	12.633	14.455	-9920(30)
$5P_{3/2}$	-1 273.78	-1 650.624	-2.663	0.881	-1652(8)
$5D_{3/2}$	-299.78	-430.540	-1.661	0.120	-432.0
$5D_{5/2}$	-125.37	-179.592	-0.841	-0.020	-180.0
$6S_{1/2}$	-11 813.60	-13 427.973	-10.131	109.116	-13328(75)
$6P_{1/2}$	-2 861.65	-3 296.683	2.062	4.505	-3290(10)
$6P_{3/2}$	-451.18	-568.727	-1.081	0.360	-569(6)
$4F_{7/2}$	-10.65	17.138	0.080	0.160	17.0
$4F_{5/2}$	-19.08	-22.083	-0.040	0.180	-22.0
$6D_{3/2}$	-136.90	-152.503	-0.701	0.200	-153.0
$6D_{5/2}$	-57.28	-64.508	-0.160	0.040	-64.0
$7S_{1/2}$	-5 333.98	-5 980.592	-5.145	48.111	-5938(16)
$7P_{1/2}$	-1 371.84	-1 548.735	0.500	1.962	-1546(6)
$7P_{3/2}$	-217.87	-273.692	-0.581	1.161	-273(4)
$5F_{7/2}$	-8.38	11.852	$\sim 0$	$\sim 0$	12.0
$5F_{5/2}$	-15.09	-29.552	-0.120	$\sim 0$	-30.0
$7D_{3/2}$	-73.87	-96.823	-0.380	-0.020	-97.0
$7D_{5/2}$	-30.93	-44.287	-0.180	0.020	-44.0
$8S_{1/2}$	-2 894.47	-3 224.987	-2.983	25.787	-3202(9)
$8P_{1/2}$	-780.91	-831.208	0.600	1.181	-829.0
$8P_{3/2}$	-124.17	-142.031	-0.240	0.060	-142.0
$8D_{3/2}$	-43.56	-56.761	-0.220	$\sim 0$	-57.0
$8D_{5/2}$	-18.27	-25.687	-0.101	$\sim 0$	-26.0
$9S_{1/2}$	-1 870.71	-2 080.223	-1.982	16.597	-2066(4)
$9P_{1/2}$	-558.97	-593.394	4.525	0.841	-588.0
$9P_{3/2}$	-88.03	-98.765	-0.681	0.040	-99.0
$9D_{3/2}$	-22.94	-29.972	-0.120	$\sim 0$	-30.0
$9D_{5/2}$	-9.63	-13.474	-0.060	$\sim 0$	-14.0

Here,  $F = I \oplus J$  with the total angular momentum of state  $J$  and the magnetic dipole hyperfine structure constant

$$A_{hyf} = \mu_N g_I \frac{\langle \Psi_v | \mathbf{O}_{hyf}^{(1)} | \Psi_v \rangle}{\sqrt{J(J+1)(2J+1)}}, \quad (21)$$

where  $\mu_N$  is the nuclear Bohr magneton,  $g_I = \frac{\mu_I}{I}$  with the nuclear magnetic moment  $\mu_I$  and  $\mathbf{O}_{hyf}^{(1)}$  is the electronic component of the spherical tensor describing the hyperfine interaction in an atomic system.

**2.3.2. Transition probability and lifetime.** The transition probability ( $A_{ik}$ ) from upper level  $i$  to lower level  $k$  is obtained from the reduced matrix elements of the electric dipole (E1) operator ( $D$ ) by using the following standard expression [57]

$$A_{ik} = \frac{2.026\ 13 \times 10^{18}}{\lambda^3} \frac{|\langle \Psi_i | \mathbf{D} | \Psi_k \rangle|^2}{g_i} \quad (22)$$

and the emission oscillator strengths are given by [57]

$$f_{ik} = -\frac{303.756}{g_i \lambda} |\langle \Psi_i | \mathbf{D} | \Psi_k \rangle|^2, \quad (23)$$

where  $\lambda$  is the transition wavelength expressed in Å,  $g_i$  is the degeneracy factor for the  $i$ th state, and  $\langle \Psi_i | \mathbf{D} | \Psi_k \rangle$  are used in atomic units (a.u.) to obtain  $A_{ik}$  in  $s^{-1}$ . From equation (23), the absorption oscillator strengths can be deduced using the relation

$$f_{ki} = -\frac{g_i}{g_k} f_{ik}. \quad (24)$$

The lifetime ( $\tau_i$ ) of the  $i$ th level is the inverse of the sum of the transition probabilities arising from all the low-lying levels and is given as

$$\tau_i = \frac{1}{\sum_k A_{ik}}. \quad (25)$$

It is to be noted here that we have neglected contributions from the forbidden channels to determine the lifetimes of the investigated atomic states as they are found to be extremely small.

**2.3.3. Dipole polarizability.** The static dipole polarizability ( $\alpha_v$ ) of an atomic state  $|\Psi_v\rangle$  with valence orbital  $v$  can be



**Table 4.** The calculated  $A_{hyf}$  values of many low-lying states of  $^{119}\text{Sn}^{3+}$  (in MHz) from the DHF and RCCSD methods are presented using the DC Hamiltonian. Corrections from the Breit interaction ( $\delta_{Breit}$ ) and QED effects ( $\delta_{QED}$ ) from the RCCSD method are also quoted. Rough estimations of uncertainties from partial excitations to some of the final results are given in parentheses. We have used  $g_I = -2.094\,56$  here.

State	DHF	RCCSD	$\delta_{Breit}$	$\delta_{QED}$	Final
$5S_{1/2}$	-40 872.69	-48 345.188	-21.322	407.350	-47959(190)
$5P_{1/2}$	-8 632.77	-10 406.235	13.216	15.123	-10378(31)
$5P_{3/2}$	-1 332.58	-1 726.818	-2.785	0.922	-1728(8)
$5D_{3/2}$	-313.61	-450.414	-1.738	0.125	-452.0
$5D_{5/2}$	-131.16	-187.882	-0.879	-0.021	-188.0
$6S_{1/2}$	-12 358.93	-14 047.816	-10.598	114.153	-13944(78)
$6P_{1/2}$	-2 993.75	-3 448.861	2.157	4.713	-3441(11)
$6P_{3/2}$	-472.00	-594.981	-1.131	0.377	-595(6)
$4F_{7/2}$	-11.14	17.929	0.084	0.167	18.0
$4F_{5/2}$	-19.96	-23.103	-0.042	0.188	-23.0
$6D_{3/2}$	-143.22	-159.542	-0.733	0.209	-160.0
$6D_{5/2}$	-59.92	-67.486	-0.167	0.042	-67.0
$7S_{1/2}$	-5 580.20	-6 256.661	-5.383	50.332	-6212(17)
$7P_{1/2}$	-1 435.17	-1 620.226	0.524	2.052	-1617(6)
$7P_{3/2}$	-227.93	-286.326	-0.607	1.215	-285(4)
$5F_{7/2}$	-8.77	12.399	$\sim 0$	$\sim 0$	12.0
$5F_{5/2}$	-15.79	-30.915	-0.125	$\sim 0$	-31.0
$7D_{3/2}$	-77.28	-101.292	-0.397	-0.021	-102.0
$7D_{5/2}$	-32.36	-46.331	-0.188	0.021	-46.0
$8S_{1/2}$	-3 028.08	-3 373.854	-3.121	26.977	-3349(9)
$8P_{1/2}$	-816.96	-869.577	0.628	1.236	-867.0
$8P_{3/2}$	-129.90	-148.588	-0.251	0.063	-149.0
$8D_{3/2}$	-45.57	-59.381	-0.230	$\sim 0$	-60.0
$8D_{5/2}$	-19.12	-26.873	-0.104	$\sim 0$	-27.0
$9S_{1/2}$	-1 957.07	-2 176.247	-2.073	17.364	-2161(4)
$9P_{1/2}$	-584.78	-620.785	4.733	0.879	-615.0
$9P_{3/2}$	-92.09	-103.325	-0.712	0.042	-104.0
$9D_{3/2}$	-24.00	-31.355	-0.126	$\sim 0$	-31.0
$9D_{5/2}$	-10.07	-14.096	-0.063	$\sim 0$	-14.0

**Table 5.** Contributions (in MHz) to  $O \equiv A_{hyf}/g_I$  values of few low-lying states in  $\text{Sn}^{3+}$ . Terms not mentioned explicitly are given together as ‘others’, and contributions from the normalization of wave functions are quoted as ‘norm’.  $\bar{O}$  means effective one-body contributions from  $e^T O e^T$  and *c.c.* denotes complex conjugate terms.

Term	$5S_{1/2}$	$5P_{1/2}$	$5P_{3/2}$	$5D_{3/2}$	$5D_{5/2}$
$O$	19 513.74	4 121.52	636.21	149.73	62.62
$\bar{O} - O$	-20.88	-3.72	4.22	2.94	1.14
$\bar{O}S_{1v} + c.c.$	2 049.18	548.75	85.40	24.41	10.18
$\bar{O}S_{2v} + c.c.$	1 599.27	315.76	77.63	28.83	14.58
$S_{1v}^\dagger \bar{O}S_{1v}$	53.87	18.35	2.86	1.00	0.42
$S_{1v}^\dagger \bar{O}S_{2v} + c.c.$	64.74	17.71	4.05	1.39	0.62
$S_{2v}^\dagger \bar{O}S_{2v}$	303.21	45.29	25.85	7.85	0.56
Others	-133.39	-27.28	-0.81	0.66	0.35
Norm	-348.43	-68.16	-10.98	-1.77	-0.77

expressed as

$$\alpha_v = -2 \sum_{v \neq k} \frac{|\langle \Psi_v | D | \Psi_k \rangle|^2}{E_v - E_k}, \quad (26)$$

be divided into three parts as

$$\alpha_v = \sum_{q=0}^2 \alpha_v^{(q)}, \quad (27)$$

where  $|\Psi_k\rangle$  represents all possible intermediate states and  $E$  denotes the energy. Carrying out tensor decomposition, it can

where  $q = 0, 1$  and  $2$  stands for scalar, vector and tensor polarizabilities, respectively. In the case of static polarizability,

**Table 6.** The DHF and RCCSD results of the BE and  $A_{hyf}/g_I$  values of the few low-lying states of Sn IV using the DC, DCB and DCQ Hamiltonians. This shows a change in the higher order relativistic effects from the DHF values due to the electron correlation effects.

Property	DC		DCB		DCQ	
	DHF	RCCSD	DHF	RCCSD	DHF	RCCSD
BE values (in $\text{cm}^{-1}$ )						
$5S_{1/2}$	315 810.90	328 953.14	315 676.22	328 802.50	315 713.41	328 847.92
$5P_{1/2}$	249 487.21	259 271.77	249 300.06	259 071.54	249 474.63	259 256.82
$5P_{3/2}$	243 519.19	252 691.32	243 411.17	253 575.50	243 525.43	252 697.19
$5D_{3/2}$	159 328.35	163 254.90	159 309.88	163 237.19	159 328.74	163 254.55
$5D_{5/2}$	158 629.08	162 499.78	158 630.35	162 502.49	158 631.59	162 501.56
$A_{hyf}/g_I$ values (in MHz)						
$5S_{1/2}$	19 513.74	23 081.31	19 495.49	23 091.49	19 347.27	22 886.83
$5P_{1/2}$	4 121.51	4 968.22	4 101.57	4 961.91	4 115.24	4 961.00
$5P_{3/2}$	636.20	824.43	634.22	825.76	636.29	823.99
$5D_{3/2}$	149.73	215.04	149.54	215.87	149.72	214.98
$5D_{5/2}$	62.61	89.70	62.57	90.12	62.62	89.71

**Table 7.** Transition rates ( $A_{ik}$ ) with the power of 10 in brackets (in  $\text{s}^{-1}$ ), absorption oscillator strengths  $f_{ki}$  (in a.u.) and transition wavelengths  $\lambda$  (in Å) for the transition from upper level  $i$  to lower level  $k$  are presented. The values of the oscillator strengths reported by Biswas *et al* [27] using the RCCSD method, and Safronova *et al* [24] using the RMBPT method, are also given along with the other literature values.

Transition		This work			$f_{ki}$		
$i$ level	$k$ level	$\lambda$	$A_{ik}$	$f_{ki}$	[27]	[24]	Others
$5P_{1/2}$	$5S_{1/2}$	1 437.527	8.235 5(8)	0.255 14	0.259	0.248 9	0.258 [21], 0.243 [20]
$6P_{1/2}$	$5S_{1/2}$	505.431	2.832 4(8)	0.010 85	0.01		
$5P_{3/2}$	$5S_{1/2}$	1 314.539	1.087 1(9)	0.563 27	0.572	0.550 8	0.567 [21], 0.538 [20]
$6P_{3/2}$	$5S_{1/2}$	499.923	1.479 0(8)	0.011 08	0.01		
$6S_{1/2}$	$5P_{1/2}$	956.252	1.165 5(9)	0.159 78	0.163		0.165 [20]
$6P_{1/2}$	$6S_{1/2}$	4 217.256	1.651 7(8)	0.440 41	0.445		
$6S_{1/2}$	$5P_{3/2}$	1 019.716	2.313 2(9)	0.180 30	0.182		0.185 [20], 0.180 [31]
$6P_{3/2}$	$6S_{1/2}$	3 862.197	2.125 7(8)	0.950 74	0.96		
$7S_{1/2}$	$5P_{1/2}$	595.055	4.892 7(8)	0.025 97	0.025		
$7S_{1/2}$	$6P_{1/2}$	2 514.787	2.726 8(8)	0.258 53	0.257		
$7S_{1/2}$	$5P_{3/2}$	619.029	9.434 1(8)	0.027 10	1.354		
$7S_{1/2}$	$6P_{3/2}$	2 660.643	5.432 3(8)	0.288 26	0.285		
$5D_{3/2}$	$5P_{1/2}$	1 044.487	2.984 2(9)	0.976 17	0.986	0.957 7	0.972 [20]
$6D_{3/2}$	$5P_{1/2}$	605.210	6.084 0(8)	0.066 82	0.036		
$5D_{3/2}$	$5P_{3/2}$	1 120.669	5.234 4(8)	0.098 56	0.111	0.096 8	0.095 [64], 0.088 [20]
$6D_{3/2}$	$5P_{3/2}$	630.027	9.017 7(7)	0.005 37	0.661		
$5D_{5/2}$	$5P_{3/2}$	1 119.338	3.136 2(9)	0.883 64	1.005	0.873 6	0.885 [20]
$6D_{5/2}$	$5P_{3/2}$	628.712	5.794 1(8)	0.051 50	5.945		
$6P_{1/2}$	$5D_{3/2}$	3 072.555	3.172 7(8)	0.224 52	0.231		
$6D_{3/2}$	$6P_{1/2}$	2 706.741	5.831 2(8)	1.280 97	1.360		
$6P_{3/2}$	$5D_{3/2}$	2 879.678	3.590 3(7)	0.044 63	0.046		
$6D_{3/2}$	$6P_{3/2}$	2 876.464	1.063 1(8)	0.131 87	0.139		
$6P_{3/2}$	$5D_{5/2}$	2 888.504	3.297 6(8)	0.274 99	0.278		
$6D_{5/2}$	$6P_{3/2}$	2 849.254	6.473 5(8)	1.181 82	1.256		
$4F_{5/2}$	$5D_{3/2}$	2 221.556	8.033 0(8)	0.891 54	0.914	0.875 1	1.036 [28]
$4F_{5/2}$	$5D_{5/2}$	2 226.804	5.748 4(7)	0.042 73	0.044	0.041 3	
$4F_{7/2}$	$5D_{5/2}$	2 229.809	8.584 1(8)	0.853 15	0.861	0.825 1	0.977 [28]
$6D_{3/2}$	$4F_{5/2}$	4 085.385	7.037 9(7)	0.117 40	0.138		
$6D_{5/2}$	$4F_{5/2}$	4 030.714	3.400 0(6)	0.008 28	0.010		
$6D_{5/2}$	$4F_{7/2}$	4 020.909	6.799 6(7)	0.123 61	0.141		



**Table 8.** Lifetimes for a few excited states (in ns) calculated in the present work and from other available literature data. The numbers in parentheses represent uncertainties. The theoretical calculations used are as follows: [24] uses RMBPT, [27] uses the RCCSD method, [28] uses the relativistic Hartree–Fock method and [31] uses Coulomb approximation, whereas the experimental results are obtained using the beam foil technique.

State	Theory		Experiment		
	Present	Others	[31]	[30]	[31]
6S <sub>1/2</sub>	0.29		0.4		0.29(4)
7S <sub>1/2</sub>	0.44				
8S <sub>1/2</sub>	0.71				
9S <sub>1/2</sub>	1.01				
5P <sub>1/2</sub>	1.21	1.2 [27], 0.95 [28], 1.26 [24]	1.03	0.73(40)	1.29(20)
5P <sub>3/2</sub>	0.92	0.9 [27], 0.74 [28], 0.95 [24]		0.93(23)	0.81(15)
6P <sub>1/2</sub>	1.31		2.2		1.41(15)
6P <sub>3/2</sub>	1.38		1.9		1.40(15)
7P <sub>1/2</sub>	1.90				
7P <sub>3/2</sub>	2.13				
8P <sub>1/2</sub>	4.89				
8P <sub>3/2</sub>	4.89				
5D <sub>3/2</sub>	0.29	0.28 [27], 0.26 [28], 0.34 [24]	0.3	0.35(3)	0.34(4)
5D <sub>5/2</sub>	0.32	0.28 [27], 0.29 [28], 0.32 [24]	0.3	0.41(3)	0.45(5)
6D <sub>3/2</sub>	0.69		0.7		1.20(25)
6D <sub>5/2</sub>	0.77		0.8		1.26(20)
4F <sub>5/2</sub>	1.12	1.0 [28], 1.13 [24]	1.1	1.05(9)	1.25(20)
4F <sub>7/2</sub>	1.17	1.1 [28], 1.38 [24]	1.1	1.06(9)	1.30(20)

vector component ( $q=1$ ) does not contribute. To carry out computations conveniently, each component  $\alpha_v^{(q)}$  of the states whose electronic configurations can be described as a closed core and a valence orbital, like in the present case, can be expressed as [58, 59]

$$\alpha_v^{(q)} = \alpha_{v,c}^{(q)} + \alpha_{v,cv}^{(q)} + \alpha_{v,v}^{(q)}, \quad (28)$$

where the notations  $c$ ,  $cv$ , and  $v$  in the subscript correspond to core, core-valence, and valence correlations, respectively. The core contributions to the tensor component of polarizability is zero. The scalar component contributes to all the atomic states whereas the tensor component contributes to the states with total angular momentum  $j > 1/2$ . It should be noted that  $\alpha_{v,v}^{(q)}$  contributes the most in the evaluation of  $\alpha_v^{(q)}$  in the considered states of  $\text{Sn}^{3+}$ . This contribution can be estimated to a very high accuracy in the sum-over-states approach using the formula

$$\alpha_{v,v}^{(0)} = 2 \sum_{k > N_c, k \neq v} W_v^{(0)} \frac{|\langle \Psi_v || \mathbf{D} || \Psi_k \rangle|^2}{E_v - E_k}, \quad (29)$$

and

$$\alpha_{v,v}^{(2)} = 2 \sum_{k > N_c, k \neq v} W_{v,k}^{(2)} \frac{|\langle \Psi_v || \mathbf{D} || \Psi_k \rangle|^2}{E_v - E_k} \quad (30)$$

with  $N_c$  as the number of occupied orbitals and the coefficients

as

$$W_v^{(0)} = -\frac{1}{3(2J_v + 1)}, \quad (31)$$

and

$$W_{v,k}^{(2)} = 2 \sqrt{\frac{5J_v(2J_v - 1)}{6(J_v + 1)(2J_v + 3)(2J_v + 1)}} \times (-1)^{J_v + J_k + 1} \begin{Bmatrix} J_v & 2 & J_v \\ 1 & J_k & 1 \end{Bmatrix}. \quad (32)$$

In the above approach, we break the valence contribution into two parts: contributions from low-lying  $k$  states up to which we can determine  $\langle \Psi_v || \mathbf{D} || \Psi_k \rangle$  matrix elements using the RCCSD method and experimental energies  $E_s$  from the Moore energy table [23], which are labeled as ‘main( $\alpha_{v,v}^{(q)}$ )’, and contributions from higher excited states, denoted as ‘tail ( $\alpha_{v,v}^{(i)}$ )’, are estimated using the DHF method. Similarly, the core-valence contributions  $\alpha_{v,cv}^{(0)}$  are also obtained using the DHF method using the expression

$$\alpha_{v,cv}^{(0)} = 2 \sum_k^{N_c} W_v^{(0)} \frac{|\langle \psi_v || \mathbf{D} || \psi_k \rangle|^2}{\epsilon_v - \epsilon_k}, \quad (33)$$

and

$$\alpha_{v,cv}^{(2)} = 2 \sum_k^{N_c} W_{v,k}^{(2)} \frac{|\langle \psi_v || \mathbf{D} || \psi_k \rangle|^2}{\epsilon_v - \epsilon_k}. \quad (34)$$

In the above expressions,  $\psi$  and  $\epsilon$  are the single particle DHF wave functions and energies, respectively. The  $\alpha_{v,c}^{(0)}$  contribution to the scalar polarizability is determined by applying the relativistic random phase approximation (RPA method) as discussed in [60].

### 3. Results and discussion

In table 1, we have provided the calculated excitation energy values (in  $\text{cm}^{-1}$ ) of many states of  $\text{Sn}^{3+}$  from the DHF and RCCSD methods. The fourth and fifth columns, respectively, represent the corrections in the excitation energy values due to the Breit interaction and QED effects. The final results along with uncertainties are quoted as ‘total’ in the same table. The uncertainties are estimated by analyzing contributions from the neglected triple excitations in the perturbative approach. From the present calculations, we see that the Breit interaction corrections to energies in  $\text{Sn}^{3+}$  are large as compared to the QED contributions, especially for the  $S_{1/2}$ ,  $P_{1/2}$  and  $P_{3/2}$  states. The contributions from these two corrections, however, have a comparable influence for the other states. This could be due to the fact that the wave functions of these states penetrate less inside the nucleus. A comparison of our theoretical EE values obtained using the RCCSD method is presented with other available theoretical calculations from the FSCC method [19] and RMBPT [24] in the same table. A reasonable agreement between our and other theoretical values is found. We compare our results for the energy levels of the considered states with the experimentally available energy data from [19] in the second last column of the same

**Table 9.** The scalar and tensor contributions (in a.u.) to the static dipole polarizabilities for the ground state and few excited states. The RPA value for the core contribution to the scalar polarizability  $\alpha_{v,c}^{(0)}$  is estimated to be 2.264 a.u. The core valence contributions are estimated to be approximately zero.  $\alpha_v^{(q)}$  values include contributions from the first few dominant transitions labeled as ‘main( $\alpha_{v,v}^{(q)}$ )’, higher excited states denoted as ‘tail( $\alpha_{v,v}^{(q)}$ )’ and core correlations  $\alpha_{v,c}^{(0)}$ .

State	Main( $\alpha_{v,v}^{(0)}$ )	Tail( $\alpha_{v,v}^{(0)}$ )	$\alpha_v^{(0)}$	Main( $\alpha_{v,v}^{(2)}$ )	Tail( $\alpha_{v,v}^{(2)}$ )	$\alpha_v^{(2)}$
5S <sub>1/2</sub>	7.27	0.02	9.53	—	—	—
6S <sub>1/2</sub>	103.57	0.03	105.85	—	—	—
7S <sub>1/2</sub>	620.25	0.02	622.58	—	—	—
8S <sub>1/2</sub>	2 078.72	0.23	2 081.20	—	—	—
9S <sub>1/2</sub>	5 866.38	0.96	5 869.59	—	—	—
5P <sub>1/2</sub>	3.48	0.04	5.78	—	—	—
6P <sub>1/2</sub>	−3.56	0.254	−1.04	—	—	—
7P <sub>1/2</sub>	161.53	1.60	−157.66	—	—	—
5P <sub>3/2</sub>	4.670	0.03	6.97	0.77	−0.026	0.74
6P <sub>3/2</sub>	10.25	0.23	12.74	20.58	−0.15	20.43
7P <sub>3/2</sub>	−78.75	1.51	−74.97	145.39	0.96	144.44
5D <sub>3/2</sub>	30.32	0.52	33.11	−11.05	−0.11	−11.16
6D <sub>3/2</sub>	286.75	1.36	290.38	−110.02	−0.31	−110.33
5D <sub>5/2</sub>	29.30	0.56	32.12	−13.82	−0.18	−13.99
6D <sub>5/2</sub>	283.18	1.54	286.98	−141.44	−0.52	−141.96

table. The values in parentheses are only due to the statistical uncertainties in their measurements, so it would be inappropriate to compare our results without actual experimental error bars. On the other hand, we notice that the other experimental measurements by Ryabtsev *et al* [22] and Moore [23] endorse our theoretical calculations very well. However, we noticed some discrepancies in the theoretical and experimental results. In table 1, the fine structure splitting of the 5D state is 733 cm<sup>−1</sup> using our method, whereas the experimental value is approximately 100 cm<sup>−1</sup>. There are two possible reasons for such large discrepancies. First, it is known that the QED corrections contribute significantly to the fine structure splitting. The QED corrections are estimated using an approximated expression in our work. Secondly, we had observed very large contributions to the energies of the D states from the electron correlation effects through triple excitation configurations through the RCC theory [61, 62]. Due to the lack of computational resources, we were unable to include these contributions in the present work. We anticipate that the inclusion of full triple excitation configurations will bring our theoretical calculations of the energies in the 5D states of Sn<sup>3+</sup> closer to the experimental results. It should be noted that exclusive-principle-violating diagrams are considered to carry out the calculations in our approach. In a complete theory, unphysical contributions arising through these diagrams are canceled through the direct and exchange terms [41]. However, these cancellations cannot be exact in an approximated method resulting in some uncertainties to the calculated quantities. These uncertainties can be minimized by considering higher level excitations in the calculations. From this point of view, we strongly believe that the inclusion of triple excitations will bring down the differences between the experimental and our calculated energy values.

The  $A_{hyf}$  values for <sup>115</sup>Sn<sup>3+</sup>, <sup>117</sup>Sn<sup>3+</sup> and <sup>119</sup>Sn<sup>3+</sup> are presented in tables 2, 3 and 4, respectively, for all the above mentioned states. We give these values from the DHF and

RCCSD methods along with the relativistic corrections from the Breit interaction and lower-order QED effects explicitly in all three isotopes. We have used  $g_I = -1.837\,66$ ,  $g_I = -2.002\,14$  and  $g_I = -2.094\,56$  for <sup>115</sup>Sn, <sup>117</sup>Sn and <sup>119</sup>Sn, respectively, to combine with our calculated  $A_{hyf}/g_I$  values to obtain the above results. As can be noticed from these tables, there are large differences between the DHF values and RCCSD values, implying quite large electron correlation contributions in the determination of these quantities. We have also quoted a rough estimation of uncertainties to some of these quantities from valence triple excitations adopting the perturbative approach. We propose experiments for the measurement of hyperfine levels of <sup>115,117,119</sup>Sn<sup>3+</sup> ions in the future to validate our calculations. These results can be further improved by considering full triple excitations in RCC theory. The  $A_{hyf}$  values for <sup>115,117,119</sup>Sn<sup>3+</sup> are theoretically provided for the first time in the present work. Sahoo *et al* has performed hyperfine structure constant calculations for Cd<sup>+</sup> using the RCCSD method [37, 63], which has a similar electronic configuration to Sn<sup>3+</sup>. The calculated  $A_{hyf}$  results for Cd<sup>+</sup> using the RCCSD method agree very well with the available experimental as well as other theoretical data. Thus, we believe the same method should give reliable results for Sn<sup>3+</sup> as well.

We also intend to demonstrate the roles of different correlation effects arising through various RCCSD terms in the evaluation of  $O = A_{hyf}/g_I$  values in Sn<sup>3+</sup>. Results only for the low-lying states 5S<sub>1/2</sub>, 5P<sub>1/2,3/2</sub> and 5D<sub>3/2,5/2</sub> are given in table 5 for illustration. It is worth stating here that the  $OS_{1v}$  and  $OS_{2v}$  RCCSD terms along with their complex conjugates (c.c.) incorporate pair-correlation and core-polarization effects to all-orders [32, 33]. In the above table, it can be seen that the DHF values (given as  $O$ ) are the largest followed by the contributions from the  $OS_{1v}$  and  $OS_{2v}$  terms. It can also be noticed that contributions from the pair-correlation effects are slightly higher than the core-polarization effects in the 5S and

$5P$  states, while it is the other way around in the  $5D$  states. We find that contributions from the non-linear terms, which are computationally expensive to account for, are also quite significant. Earlier studies of hyperfine structure constants in the  $D_{5/2}$  states of singly-charged alkaline earth-metals [34] and of alkali atoms (for example, the Fr atom in [35]) show unusual behavior in contrast to the other states. For instance, it shows a large contribution from  $OS_{2v}$ , even larger than the DHF value with an opposite sign. However, the correlation trend in the evaluation of  $A_{hyf}/g_I$  in the  $5D_{5/2}$  state follows a similar pattern as the other states in  $\text{Sn}^{3+}$ .

To demonstrate changes in the contributions of the Breit and QED interactions in the calculated quantities due to the electron correlation effects, we present the BE and  $A_{hyf}/g_I$  values of the above five selected states in table 6 from the DHF and RCCSD methods considering DC, DCB, and DCQ Hamiltonians. As can be seen, the electron correlation effects change these relativistic effects significantly to both the above quantities.

Transition probabilities for as many as 155 transition lines are obtained for  $\text{Sn}^{3+}$  in our present work. A few of these transitions, for which a comparison from previous literature is available, are listed in column 4 of table 7. The transition probabilities for other transitions are tabulated in the supplementary material (available online at [stacks.iop.org/JPB/53/065002/mmedia](https://stacks.iop.org/JPB/53/065002/mmedia)). In the same table, we also present the corresponding absorption oscillator strengths ( $f_{ki}$ ) from the present work and previously reported theoretical values from [27] in columns 5 and 6 respectively. Our calculated values of oscillator strengths are also compared with the previously reported theoretical results by Safronova *et al* [24] and other literature in the last two columns of the same table. The oscillator strengths calculated by Biswas and co workers [27], who also use the RCCSD method, are generally in good agreement with our results, but unusually large discrepancies were found among a few transitions. For instance, the oscillator strength values for the  $5D_j - 5P_{3/2}$  transition by them differ from our calculations by approximately 12% and 14% respectively. A similar inconsistency is observed for  $6D_j - 5P_{j'}$  oscillator strengths. These discrepancies are attributed to the disagreement in the matrix element values for these transitions (see table 1 in the supplementary material for a comparison of matrix elements). A close inspection of the oscillator strengths of transitions  $7S_{1/2} - 5P_{1/2,3/2}$  and  $7S_{1/2} - 6P_{1/2,3/2}$  given by Biswas *et al* [27] points out that results for the  $7S_{1/2} - 6P_{3/2}$  transition are not correct due to the following simple reason. Assuming that the radial component of the wave functions between the  $5P_{1/2}$  and  $5P_{3/2}$  states and also between the  $6P_{1/2}$  and  $6P_{3/2}$  states are almost similar, the E1 matrix elements between the  $7S_{1/2} - 5P_{1/2}$  and  $7S_{1/2} - 5P_{3/2}$  transitions and also between the  $7S_{1/2} - 6P_{1/2}$  and  $7S_{1/2} - 6P_{3/2}$  transitions should differ mainly because of the angular factors. As seen, both we and Biswas *et al* [27] have obtained similar matrix elements between the  $7S_{1/2} - 6P_{1/2}$  and  $7S_{1/2} - 6P_{3/2}$  transitions, which differ by one and half times approximately. Therefore, a similar factor difference between the E1 matrix elements of the transitions  $7S_{1/2} - 5P_{1/2}$  and  $7S_{1/2} - 5P_{3/2}$  is expected.

We believe that our results are more reliable as they have been improved recently [53, 54] and our calculations match well with the other available literature. For the  $5D_j - 5P_{j'}$  transitions, the oscillator strengths are in agreement with the values given in [20], which are evaluated using the core-potential in the Dirac–Fock (DFCP) method. In [21], oscillator strengths for the  $5P_j - 5S_{1/2}$  transitions are calculated employing the CI method and our values are in good agreement with their numbers. We notice a remarkable agreement between our results and the values calculated in [24] using RMBPT. Our oscillator strengths for the  $4F_{5/2} - 5D_{3/2}$  and  $4F_{7/2} - 5D_{5/2}$  transitions are not in agreement with the results from the calculations of Cheng and Kim [28]. They used the relativistic Hartree–Fock method whereas our calculations are based on the RCC method which includes correlation corrections to all orders. Our oscillator strength for the  $6S_{1/2} - 5P_{3/2}$  transition is very close to the experimental result of Pinnington *et al* [31], which is measured using the beam foil technique.

In table 8, the estimation of the lifetimes for the ground and few excited states along with a comparison with other available literature is presented. The theoretical calculations for the lifetimes of various states are available in [24, 27, 28, 31]. In [27], the authors use the RCCSD method, whereas the RMBPT and DFCP methods are employed for the calculations in [24] and [28] respectively. Theoretical calculations from [31] are obtained assuming LS coupling and Coulomb-approximation radial wave functions. In general, Coulomb approximation is only strictly valid for highly excited states with non-penetrating wave functions. Hence, it is not a match for our sophisticated calculations using the RCCSD method. Our calculations match very well with these theoretical results. Experimental lifetime measurements for some states of  $\text{Sn}^{3+}$  using the beam foil technique are available in the literature [30, 31]. Our calculations mostly show agreement with the experimental results within the experimental uncertainties except for discrepancies in a few places. We notice discrepancies between our lifetime calculations and measurements from Pennington [31] for the  $5D$  and  $6D$  states. Similarly, our results for the  $5P_{1/2}$  and  $5D$  states are not consistent with the measurements in [30], but they match well with other theoretical and experimental investigations. Perhaps including correlation corrections from the triple excitations can remove these discrepancies. Therefore, it calls for more theoretical and experimental investigations for the lifetimes of these states in  $\text{Sn}^{3+}$ .

In table 9, the calculated values of the static scalar dipole polarizabilities for  $nS_{1/2}$  ( $n = 5-9$ ),  $nP_{1/2, 3/2}$  ( $n = 5-7$ ) and  $nD_{3/2,5/2}$  ( $n = 5, 6$ ) are listed. In the same table, the values of the static tensor dipole polarizabilities for  $nP_{3/2}$  ( $n = 5-7$ ) and  $nD_{3/2,5/2}$  ( $n = 5, 6$ ) are also tabulated. The dominant ‘main’ contributions to the valence correlation for the scalar and tensor dipole polarizabilities are presented along with the ‘tail’ parts. The core contribution has been calculated using RPA and is found to be 2.264 a.u. The contributions of the valence core correlations are found to be very small and thus they have been excluded from the table. It is found in our

calculations that  $\text{Sn}^{3+}$  in its ground state will not respond much to the electric field as shown by a small value of static scalar polarizability ( $\alpha_v^{(0)} = 9.53$  a.u.). This small  $\alpha_v^{(0)}$  value is owing to the very large energy differences between the ground and  $5P$  states leading to much less contribution to the polarizability from the primary  $5S_{1/2} - 5P_{1/2,3/2}$  transitions.

## 4. Conclusion

In summary, the theoretical results of the energies, magnetic dipole hyperfine structure constants and electric dipole matrix elements of many low-lying states of the  $\text{Sn}^{3+}$  are presented. Transition probabilities and oscillator strengths of 155 spectral lines arising from the  $nS_{1/2}(n = 5 - 9)$ ,  $nP_{1/2,3/2}(n = 5 - 9)$ ,  $nD_{3/2,5/2}(n = 5 - 9)$  and  $nF_{5/2,7/2}(n = 4,5)$  states along with radiative lifetimes for the 18 levels and static dipole polarizabilities of the 15 states have been determined. These values were obtained by employing relativistic couple-cluster theory with single and double excitation approximation. The estimated transition probabilities, oscillator strengths, and radiative lifetimes are generally found to be in good agreement with the available experimental data. The reported polarizability results for  $\text{Sn}^{3+}$  can be useful in estimating systematics for carrying out high precision spectroscopic measurements in this ion.

## Acknowledgments

The work of BA is supported by DST-SERB Grant No. EMR/2016/001228. BKS would like to acknowledge the use of the Vikram-100 HPC cluster facility of the Physical Research Laboratory, Ahmedabad, India.

## ORCID iDs

B K Sahoo  <https://orcid.org/0000-0003-4397-7965>

## References

- [1] Berengut J C, Dzuba V A and Flambaum V V 2010 *Phys. Rev. Lett.* **105** 120801
- [2] Kozlov M G, Safronova M S, Crespo López-Urrutia J R and Schmidt P O 2018 *Rev. Mod. Phys.* **90** 045005
- [3] Yu Y-M and Sahoo B K 2016 *Phys. Rev. A* **94** 062502
- [4] Yu Y-M and Sahoo B K 2018 *Phys. Rev. A* **97** 041403
- [5] Bloom B J, Nicholson T L, Williams J R, Campbell S L, Bishof M, Zhang X, Zhang W, Bromley S L and Ye J 2014 *Nature* **506** 71–5
- [6] Hinkley N, Sherman J A, Phillips N B, Schioppo M, Lemke N D, Beloy K, Pizzocaro M, Oates C W and Ludlow A D 2013 *Science* **341** 1215
- [7] Sterling N C, Dinerstein H L and Bowers C W 2002 *Astrophys. J.* **578** L55–8
- [8] Savage B D and Sembach K R 1996 *Annu. Rev. Astron. Astrophys.* **34** 279
- [9] Monchinsky V, Kalagin I and Govorov A 1996 *Laser Part. Beams* **14** 439442
- [10] Tomie T 2012 *J. Micro/Nanolithogr. MEMS MOEMS* **11** 1
- [11] White J, Hayden P, Dunne P, Cummings A, Murphy N, Sheridan P and O'Sullivan G 2005 *J. Appl. Phys.* **98** 113301
- [12] Attwood D 1999 *Soft X-Rays and Extreme Ultraviolet Radiation Principles and Applications* (Cambridge: Cambridge University Press)
- [13] Banine V Y, Koshelev K N and Swinkels G H P M 2011 *J. Phys. D* **44** 253001
- [14] Svendsen W and O'Sullivan G 1994 *Phys. Rev. A* **50** 3710–8
- [15] Peth C, Barkusky F and Mann K 2008 *J. Phys. D* **41** 105202
- [16] Barkusky F, Bayer A, Döring S, Grossmann P and Mann K 2010 *Opt. Express* **18** 4346
- [17] Kieft E R, van der Mullen J J A M, Kroesen G M W, Banine V and Koshelev K N 2004 *Phys. Rev. E* **70** 066402
- [18] Namba S, Fujioka S, Sakaguchi H, Nishimura H, Yasuda Y, Nagai K, Miyana N, Izawa Y, Mima K and Sato K 2008 *J. Appl. Phys.* **104** 013305
- [19] Scheers J et al 2018 *Phys. Rev. A* **98** 062503
- [20] Migdalek J and Garmulewicz M 2000 *J. Phys. B: At. Mol. Opt. Phys.* **33** 1735–43
- [21] Glowacki L and Migdalek J 2009 *Phys. Rev. A* **80** 042505
- [22] Ryabtsev A N, Churilov S S and Kononov E Y 2006 *Opt. Spectr. (USSR)* **100** 652
- [23] Moore C 1958 *Atomic Energy Levels III* (Gaithersburg, MD: National Bureau of Standards)
- [24] Safronova U I, Savukov I M, Safronova M S and Johnson W R 2003 *Phys. Rev. A* **68** 062505
- [25] Su M G, Min Q, Cao S Q, Sun D X, Hayden P, O'Sullivan G and Dong C Z 2017 *Sci. Rep.* **7** 45212
- [26] Safronova M S, Dzuba V A, Flambaum V V, Safronova U I, Porsev S G and Kozlov M G 2014 *Phys. Rev. Lett.* **113** 030801
- [27] Biswas S, Bhowmik A, Das A and Majumder S 2018 *Mon. Not. R. Astron. Soc.* **477** 5605–11
- [28] Cheng K T and Kim Y K 1979 *J. Opt. Soc. Am.* **69** 125–31
- [29] Andersen T, Nielsen A K and Sørensen G 1972 *Phys. Scr.* **6** 122–4
- [30] Kernahan J A, Pinnington E H, Ansbacher W and Bahr J L 1985 *Nucl. Instrum. Methods Phys. Res. B* **9** 616
- [31] Pinnington E H, Kernahan J A and Ansbacher W 1987 *Can. J. Phys.* **65** 7
- [32] Sahoo B K, Gopakumar G, Merlitz H, Chaudhuri R K, Das B P, Mahapatra U S and Mukherjee D 2003 *Phys. Rev. A* **68** 040501(R)
- [33] Sahoo B K, Chaudhuri R K, Merlitz H, Das B P and Mukherjee D 2005 *Phys. Rev. A* **72** 032507
- [34] Sahoo B K, Sur C, Beier T, Das B P, Chaudhuri R K and Mukherjee D 2007 *Phys. Rev. A* **75** 042504
- [35] Sahoo B K, Nandy D, Das B P and Sakemi Y 2015 *Phys. Rev. A* **91** 042507
- [36] Sahoo B K 2009 *Phys. Rev. A* **80** 012515
- [37] Yu Y-M and Sahoo B K 2017 *Phys. Rev. A* **96** 050502(R)
- [38] Itano W M 2000 *J. Res. Natl. Inst. Stand. Technol.* **105** 829
- [39] Sahoo B K 2017 *Relativistic Calculations of Atomic Clock (Handbook of Relativistic Quantum Chemistry)* ed W Liu (Berlin: Springer)
- [40] Tolansky S and Forester G O 1941 *London, Edinburgh, Dublin Phil. Mag. J. Sci.* **32** 315
- [41] Lindgren I and Morrison J 1982 *Atomic Many-Body Theory* (Berlin: Springer)
- [42] Coenen J W, Temmerman G D, Federici G, Philipps V, Sergienko G, Strohmayer G, Terra A, Unterberg B, Wegener T and Van den Bekerom D C M 2014 *Phys. Scr.* **T159** 014037
- [43] van Eden G G, Morgan T W, Aussems D U B, van den Berg M A, Bystrov K and van de Sanden M C M 2016 *Phys. Rev. Lett.* **116** 135002

- [44] van Eden G G, Kvon V, van de Sanden M C M and Morgan T W 2017 *Nat. Commun.* **8** 192
- [45] Lunt J 1907 *Mon. Not. R. Astron. Soc.* **67** 487
- [46] O'Toole S J 2004 *Astron. Astrophys.* **423** L25–8
- [47] Vennes S, Chayer P and Dupuis J 2005 *Astrophys. J.* **622** L121–4
- [48] Sofia U J, Meyer D M and Cardelli J A 1999 *Astrophys. J. Lett.* **522** L137–40
- [49] Hobbs L M, Welty D E, Morton D C, Spitzer L and York D G 1993 *Astrophys. J.* **411** 750–5
- [50] Proffitt C R, Sansonetti C J and Reader J 2001 *Astrophys. J.* **557** 320
- [51] Chayer P, Vennes S, Dupuis J and Kruk J W 2005 *Astrophys. J. Lett.* **630** L169–72
- [52] Nandy D K and Sahoo B K 2014 *Phys. Rev. A* **90** 050503(R)
- [53] Sahoo B K and Das B P 2015 *Phys. Rev. A* **92** 052511
- [54] Sahoo B K, Nandy D K, Das B P and Sakemi Y 2015 *Phys. Rev. A* **91** 042507
- [55] Uehling E A 1935 *Phys. Rev.* **48** 55–63
- [56] Ginges J S M and Berengut J C 2016 *Phys. Rev. A* **93** 052509
- [57] Sobelman I I 1979 *Atomic Spectra and Radiative Transitions* (Berlin: Springer)
- [58] Kaur J, Nandy D K, Arora B and Sahoo B K 2015 *Phys. Rev. A* **91** 012705
- [59] Arora B, Nandy D K and Sahoo B K 2012 *Phys. Rev. A* **85** 012506
- [60] Singh Y and Sahoo B K 2014 *Phys. Rev. A* **90** 022511
- [61] Sahoo B K 2019 *Phys. Rev. A* **99** 050501(R)
- [62] Sahoo B K 2016 *Phys. Rev. A* **93** 022503
- [63] Li C-B, Yu Y-M and Sahoo B K 2018 *Phys. Rev. A* **97** 022512
- [64] Migdalek J and Baylis W E 1979 *J. Quant. Spectrosc. Radiat. Transfer* **22** 113–25